Available online at www.sciencedirect.com

SCIENCE DIRECT®

Geomorphology 63 (2004) 57–80

GEOMORPHOLOGY

www.elsevier.com/locate/geomorph

Landslide-induced river channel avulsions in mountain catchments of southwest New Zealand

Oliver Korup*

School of Earth Sciences, Victoria University of Wellington, P.O. Box 600, New Zealand

Received 3 April 2003; received in revised form 19 March 2004; accepted 22 March 2004
Available online 20 May 2004

Abstract

Pulsed or chronic supply of landslide debris to valley floors has historically caused substantial aggradation and channel instability in several alpine catchments of SW New Zealand. In this regional investigation of landslide impacts on river morphology, three types of landslide-induced channel avulsion are discerned: (i) upstream/backwater avulsions, (ii) contact avulsions, and (iii) downstream/loading avulsions. The basis for this qualitative geomorphic process-response framework is the principal direction of fluvial response with respect to its position relative to the causative landslide emplacement site. Downstream avulsions have the highest damage potential to land use and infrastructure on unconfined mountain-fringe alluvial fans. In the wake of such events, catastrophic aggradation may obliterate up to several km^2 of mature floodplain forests by burial under several metres within a few decades. Estimates of mean aggradation rates are high (<220 mm $year^{-1}$) and exceed long-term (10^3 year) trends of fluvial degradation by an order of magnitude. Future potential avulsion routeways may be detected by geomorphic mapping of abandoned channels, which are preferentially reactivated in the wake of landslide-induced sediment waves.

Keywords: Avulsion; River channel; Landslide; Channel–hillslope coupling; Aggradation

1. Introduction

The natural variability of water and sediment discharge in mountain rivers is high and often difficult to measure or predict (Kirchner et al., 2001). To ensure sustainable long-term planning and development, the morphodynamics of mountain rivers need to be understood not only during single events such as flash floods (ICIMOD, 2000), but also during high sediment loads maintained over years or decades. Catastrophic or chronic sediment input from large landslides may be one of various causes that pose substantial problems to engineering and land management. Excessive valley-floor aggradation promotes increases in flood frequency, channel instability, potential damage to housing, infrastructure or land use activities, conveyance of pollutants, and general deterioration of aquatic habitats (Anthony and Julian, 1999; Miller and Benda, 2000; Sutherland et al., 2002; Clague et al., 2003). Alpine rivers that debouch onto unconfined foreland plains commonly deposit high amounts of bed-load sediment at mountain-range fronts. Such is the case for the West Coast of South

* Present address: WSL Swiss Federal Institute for Snow and Avalanche Research SLF, Flüelastr. 11, CH-7260 Davos, Switzerland. Tel.: +41-814-170354; fax: +41-814-170010.
E-mail address: korup@slf.ch (O. Korup).

0169-555X/$ - see front matter © 2004 Elsevier B.V. All rights reserved.
doi:10.1016/j.geomorph.2004.03.005

Island, New Zealand, where settlements and a major highway are located on mountain-fringe alluvial fans fed by steep rivers with extremely high specific mean annual floods and sediment yields (McKerchar and Pearson, 1989; Hicks et al., 1996).

This paper addresses the geomorphic impact of landslides on large-scale river channel stability in alpine South Westland and Northern Fiordland, New Zealand. Its main objectives are:

1. To present evidence of three major historic landslide-initiated channel avulsions and to place them—along with further regional evidence—within a typology;
2. To assess the suitability of (a) geomorphometric scaling relationships, (b) sediment input, and (c) geomorphic process response as the conceptual basis for such a typology; and
3. To assess fluvial response and recovery by comparing mean process rates associated with landslide-induced channel avulsions with long-term trends of fluvial incision.

2. Previous work on landslide-induced channel avulsions

Channel avulsion is defined as the rapid lateral relocation of a river course across parts of its floodplain due to changes in local valley slope (Jones and Schumm, 1999). In braided gravel-bed rivers common to many mountain catchments, the process of channel avulsion differs from that of lateral migration as it involves the shifting of channel trains rather than single braids (Nanson and Knighton, 1996). Although there is a considerable body of literature on the processes and forms involved with channel avulsions, few studies have dealt explicitly with the effect of landslide-induced avulsions, "diversions", or "restrictions" (Ohmori, 1992; Bartarya and Sah, 1995; Sah and Mazari, 1998; Shroder, 1998; Ritter et al., 1999; Paul et al., 2000). Heim (1932) included a sketch of a "Flussverschiebung durch Bergsturz", i.e. landslide-induced channel diversion or deflection, in his pioneering classification of mass movement in the European Alps. Indirect information can be gathered from literature on landslide dams, which are morphogenetically related to the phenomenon of landslide-induced river avulsions, especially with regard to the formation of breach or spillway channels (Hewitt, 1998). In New Zealand, a benchmark study by Griffiths and McSaveney (1986) estimated specific sediment yields from fan aggradation following a historic landslide-induced avulsion on the Waitangitaona River, South Westland.

3. Study area

The study area in SW New Zealand roughly comprises the northern and central portions of the 2.6×10^4 km^2 Te Waahipounamu World Heritage area (42°57′ –46°16′ S, 166°25′ –170°56′ E). It contains the fault-bounded mountain–foreland complex of South Westland and northern Fiordland (Fig. 1).

The Alpine Fault is the dominant structural feature marking the active oblique convergence of the Indo-Australian and Pacific plates. The western slopes of the Southern Alps collisional orogen constitute the hanging wall of the dextral transpressional fault and attain elevations of nearly 3700 m a.s.l. over a horizontal distance of 20–30 km. Coseismic uplift and dissection by steep and closely spaced mountain rivers west of the Main Divide have unroofed metamorphic Haast Group Schist (Norris and Cooper, 2000). Rivers debouch onto extensive alluvial plains fringed by Pleistocene lateral moraine ridges and hilly outcrops of Ordovician basement (Nathan, 1978). Northern Fiordland is characterized by a glacial trough and fjord landscape cut into crystalline basement rocks, with oblique convergence changing to offshore subduction. The SW–NE striking mountain ranges block moist northwesterly airflow, causing extreme orographic precipitation of up to 14,000 mm year^{-1} near the Main Divide and coastal Fiordland (Henderson and Thompson, 1999). Throughout the study area, steep rectilinear hillslopes are subject to extensive landsliding (Hovius et al., 1997). High local relief and low accommodation space on alpine valley floors promote frequent geomorphic coupling and delivery of landslide debris to river channels. Vegetation is prolific and largely dominated by Podocarpaceae and *Nothofagus* mountain rainforests. Despite the remoteness of the area, several Westland rivers have been prospected and sluiced for alluvial gold during the 1860s (Craw et al., 1999).

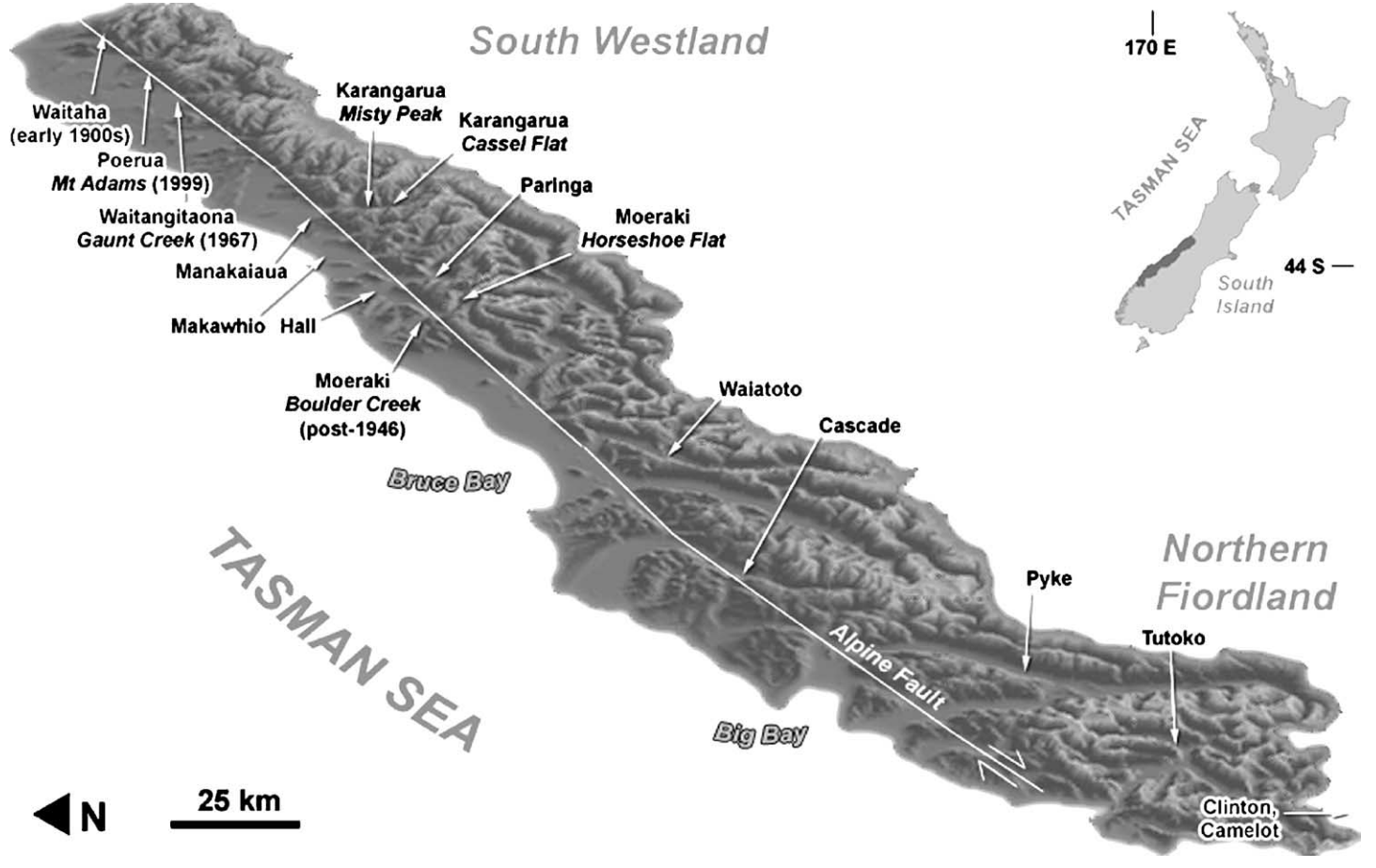

Fig. 1. Shaded relief of South Westland and northern Fiordland, New Zealand, as seen from W. Arrows indicate major channel avulsions on mountain-fringe alluvial fans and intramontane valley trains of alpine rivers (known avulsion ages are bracketed). Note the linear trace of the Alpine Fault separating the Southern Alps from the subdued foreland.

4. Methods

Over 3000 multi-temporal air photos covering the mountainous SW of New Zealand were inspected to detect and map various forms of landslide-induced river disruption such as blockage, occlusion, excessive debris input, and channel avulsions. During this regional reconnaissance, 250 landslides affecting a total area of ~370 km^2 were mapped and stored in a GIS landslide inventory (Korup, 2003). This study focuses on some of those slope failures found to be associated with major channel avulsions (Fig. 1). Scars in the dense vegetation cover (e.g. highly reflective gravel patches, distinctive contrasts in growth height) were found to be ideal for detecting avulsions from air photos. Avulsion and aggradation traces were mapped from air photos onto a digital version of the New Zealand Map Series 260 (NZMS260) at 1:50,000 scale. Landslide polygons depicting total affected area were intersected with a 25-m cell-size DEM to extract geomorphometric attributes for failure sites and upstream catchments. Other attributes such as, for example, the length of the geomorphic coupling interface between landslide and river channel were mapped directly onto the GIS. Fieldwork included validation of air photo interpretation; observations and descriptions of riverbed forms at various stages of aggradation and degradation (Fig. 2); (repeated) surveys of selected channel and alluvial fan cross-sections with an Electronic Distance Meter (EDM); and mapping of (dendro-)geomorphic features with a handheld 12-channel GPS receiver (x,y resolution of ±2 m). Detailed logs of geomorphic, morphostratigraphic and dendrogeomorphic evidence were obtained from natural river bank exposures and exhumed in situ tree cohorts. Particle size of bed-load sediment was sampled and determined in the field using calliper and tape measure. Published data on sediment yields and geomorphic process rates in the region were reviewed and augmented with personal observations.

5. Examples of historic landslide-induced channel avulsions in South Westland

Three major channel avulsions resulted from disturbances by large-scale slope instability in South Westland during the 20th century. Event sequences are well-documented on air photos and are summarized here together with geomorphic evidence.

5.1. Gaunt Creek, Waitangitaona River

Gaunt Creek is a small tributary of the Waitangitaona River, which drains ~73 km^2 of the mountain range front along the Alpine Fault (Fig. 1). Chronic slope instability at a site referred to in the following as "Gaunt Creek Slip" had caused high debris input and downstream aggradation since ~1918 (Fig. 3). This culminated in March 1967, when a minor flood triggered an avulsion of the Waitangitaona River on its mountain-fringe alluvial fan near the State Highway 6 (SH6) bridge, shifting the river's original seaward course towards Lake Wahapo in the Okarito River catchment (Griffiths and McSaveney, 1986). The avulsion channel formed on a braided fan-delta complex (Goedhart and Smith, 1998), which gradually buried ~3.7 km^2 of swamp and farmland.

Gaunt Creek Slip is a large (~0.34 km^2) gully/landslide complex in highly brittle and readily erodible Haast Schist-derived mylonite, cataclasite, and Alpine Fault gouge (Fig. 3). The detailed lithological and tectonic setting of this significant exposure were described by Cooper and Norris (1994). Low shrub vegetation covers most of the complex (as of 2003), although debris slide, slump, fall, and topple, slope wash, rill and gully erosion, as well as fluvial undercutting, maintain sporadic sediment input to Gaunt Creek. Dip projection of tributary fan surfaces opposite Gaunt Creek Slip suggests former occlusion of Gaunt Creek by debris flow deposits (OC, Fig. 3), forcing lateral channel shift and subsequent undercutting of the fault zone.

Gaunt Creek occupies a ~2.7-km^2 low-angle fan (gradient ~0.035) covered by pristine and second-growth podocarp forest. Landslide-induced aggradation had affected ~28% of the fan area in the late 1940s, causing burial of ~0.1 km^2 of mature forest during a major avulsion (GA, Fig. 3) and formation of a small telescope fan. Subsequent incision of up to ~8 m is recorded in several flights of terraces along unpaired cut-and-fill fan cross-sections. A vegetation chronosequence from red algae, fruticose lichen, several grass species, to shrubs and juvenile rimu (*Dacrydium cupressinum*) trees supports the relative surface

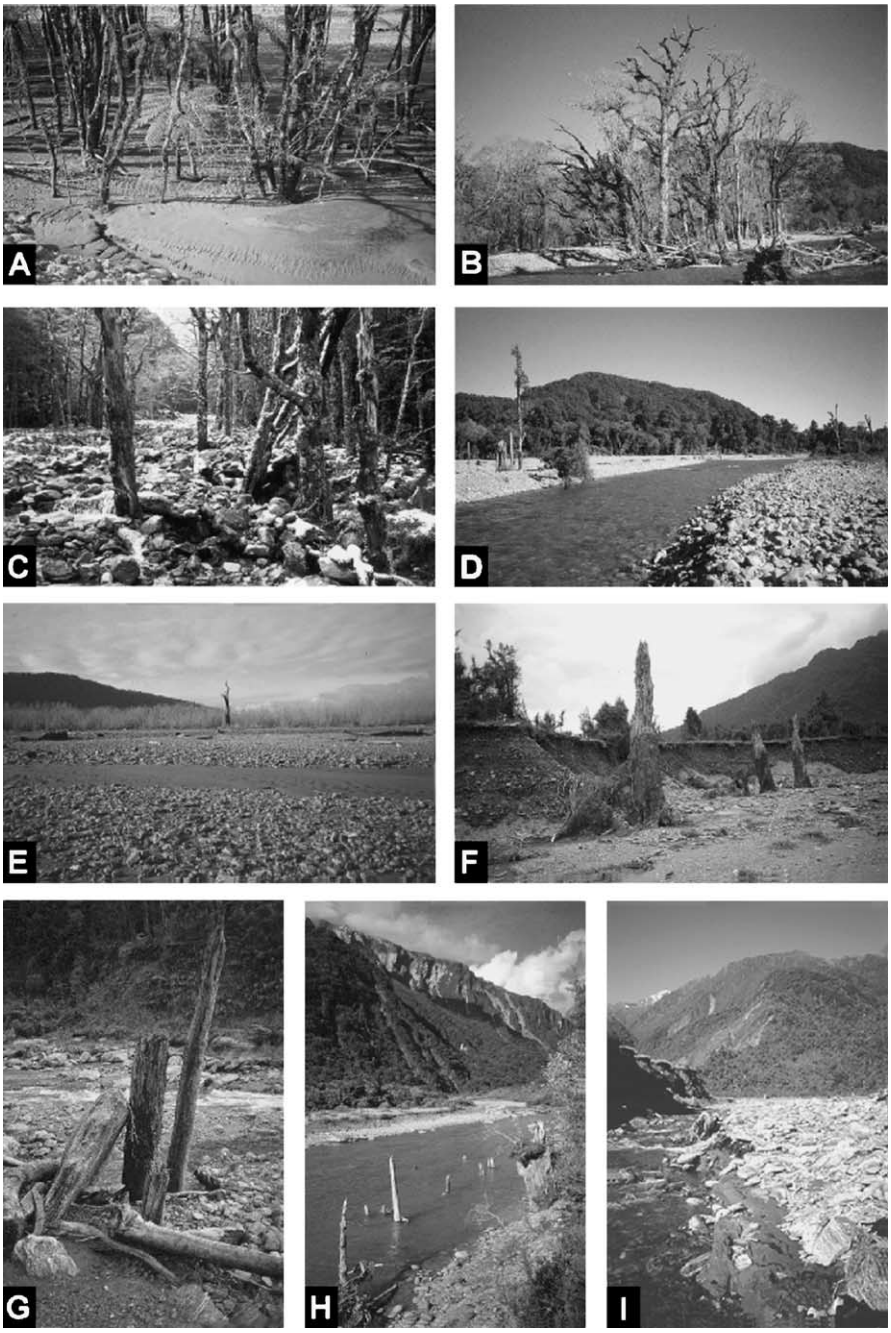

Fig. 2. Stages of aggradation-induced die-back in floodplain forests of South Westland and Fiordland. (A) Burial of undergrowth on distal active braidplain, Waiho River; (B) partly degraded *Nothofagus* trees on buried floodplain, Moeraki River; (C) in-channel destruction of *Nothofagus* trees, Borland Burn; (D) channel establishment on formerly stable floodplain, Moeraki River; (E) active mid-fan aggradation with remnant stands of former floodplain vegetation, Waitangitaona River; (F) re-exhumed in situ tree stumps, Gaunt Creek Fan; (G) rotated large woody debris in mid-channel position, Darnley Creek; (H) re-exhumation of in situ tree cohort at Welcome Flat, Copland River; (I) re-exhumed truncated forest soil with in situ tree stumps, Gaunt Creek. Note that (A), (G), and (H) are not necessarily related to landslide-induced aggradation.

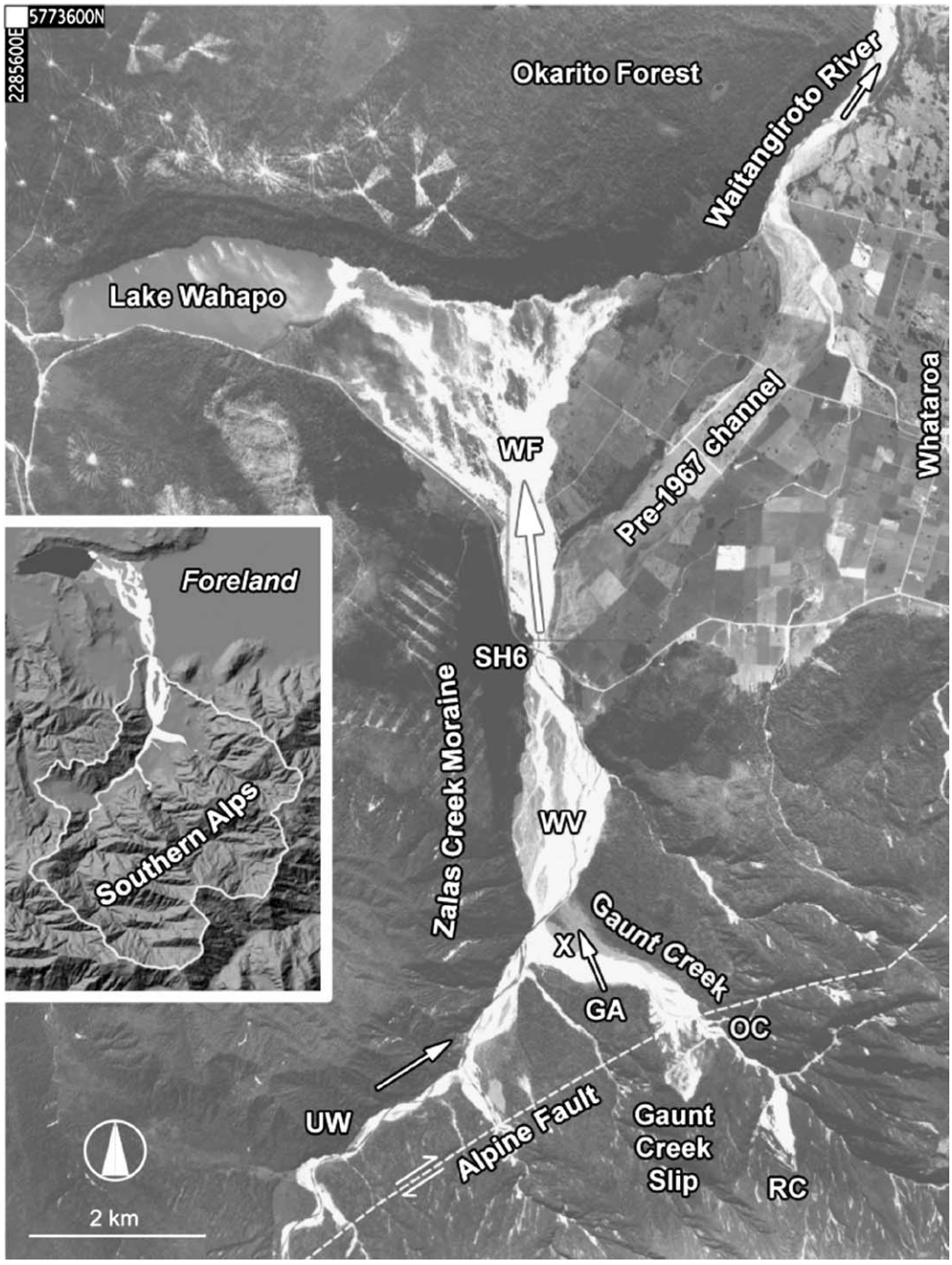

Fig. 3. Landslide-driven avulsion on Waitangitaona River, South Westland. Inset shaded relief map shows Waitangitaona catchment boundary. GA=Gaunt Creek avulsion; OC=channel occlusion at Gaunt Creek fan apex; RC=ridge crest failure developed in 1980s; SH6=State Highway 6 bridge; UW=Upper Waitangitaona River; WF=Waitangitaona terminal fan; WV=Lower Waitangitaona River valley train; X=location of section in Fig. 5. Image courtesy of Land Information New Zealand (SN8493/E13, Crown©); coordinates refer to New Zealand Map Grid.

age and stability inferred from air photos. A thinned cohort of dead tree stumps in situ records historic aggradation on the SW distal portions of the fan. There, perched remnants of aggradation surfaces are lodged in small clusters of live rimu. Several cobble nests in major branches of tree trunks up to 5.2 m above the present fan surface indicate minimum burial depths (see Fig. 4 for an example with a relative height of 2.5 m). These remnants correspond well with three distinctive terrace treads, which were identified in the field and on air photos between 1948 and 1987. Remnants of buried forest soils in the present channel bed on the distal N parts of the fan support evidence of rapid aggradation/degradation of 2–5 m within ~40 years (Fig. 2F,I).

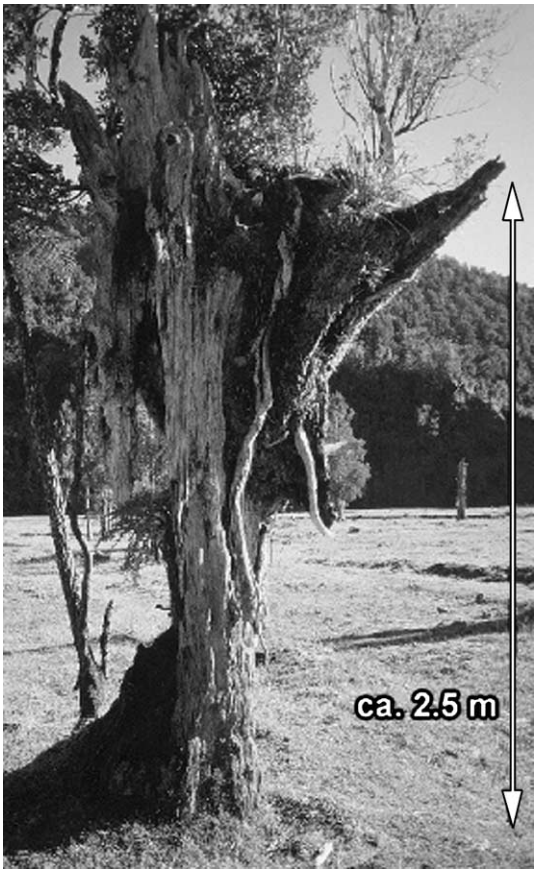

Fig. 4. (Dendro-)geomorphic evidence of historic landslide-driven aggradation at Gaunt Creek, Waitangitaona River: exhumed tree stump hosts perched cobble nests as remnants of historic aggradation surfaces.

All palaeosols are truncated and devoid of topsoil, and contain root beds, partly decomposed wood fragments, and few in situ tree stumps. Terrace risers contain several buried soil horizons towards the distal portion of the fan, while mid-fan stratigraphy exhibits sheets of crudely bedded gravel <8 m thick (Fig. 5). The combination of temporal brackets from air photo on the timing of aggradation pulses with survey data suggests that Gaunt Creek Fan has undergone a net loss of $\sim 3.5 \times 10^6$ m^3 since peak aggradation in ~1965. This translates to a subsequent mean degradation rate of ~150–220 mm year^{-1} along the fan.

The Waitangitaona River downstream of the Gaunt Creek confluence (WV, Fig. 3) occupies a broad gravel-bed floodplain bounded by the trimmed toes of Gaunt Creek Fan and the Zalas Creek moraine (Griffiths and McSaveney, 1986). Air photos show at least two major avulsions following the passing of major sediment waves (Nicholas et al., 1995) since the 1940s. Reduction of active channel area from 70% to 47% between 1978 and 1987 possibly reflects the recovery from the sediment pulse. Scour and decomposition marks on buried and re-excavated trees in situ on the true left floodplain margin some 500 m upstream of the SH6 bridge record historic aggradation of ~1.8 m.

At SH6, the Waitangitaona River debouches onto a large terminal fan, which has been reactivated as a result of the 1967 avulsion (WF, Fig. 3). The establishment of the avulsion channel through laterally unconfined farmland and swamp forests is characterized by several prograding gravel lobes and floodouts (Fig. 6).

Maximum advance rates of 0.8–1.0 km year^{-1} mark the morphodynamic adjustment process to a 55% reduction of effective channel width. More than 3 years after the avulsion the lobe fronts had reached the NE shores of Lake Wahapo, gradually forming two fan-toe deltas. Profile lengthening caused subsequent fan-head trenching by fluvial scour. This undermined parts of the SH6 bridge foundations in 1982 (Griffiths and McSaveney, 1986). The increased discharge into Lake Wahapo has facilitated use of a small hydropower plant, whereas major stopbanks had to be erected on the fan in the mid-1980s to reduce the possibility of another avulsion of the Waitangitaona River towards its former course. Artificial lateral constriction has favoured a perched bed level of ~2 m above the

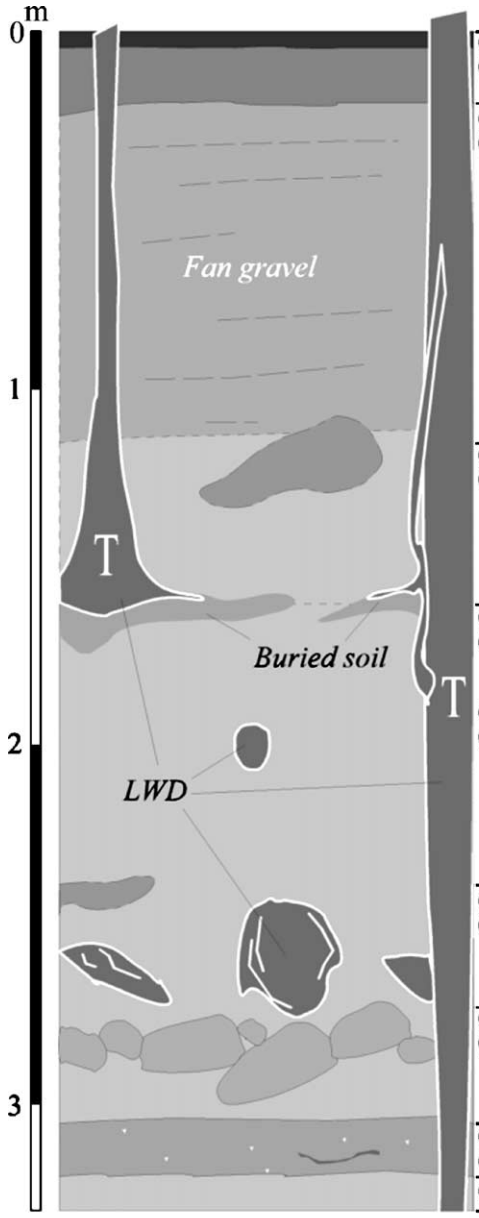

NZMG 2291807E 5768065N

GC I (0-20 cm)	Grass, root mat with young to mature trees; med. coarse pebbles in massive matrix of very dark grey (5Y 3/1) ~5 cm weakly developed humic topsoil (mod. well sorted fine loamy sand; high root cohesion
GC II (20-115 cm)	Black (5Y 3/1, 5Y 2.5/1) crudely bedded (downstream-dipping), poorly sorted angular to subangular clast-supported very coarse pebbles to fine cobbles; lenses of med. to coarse pebbly coarse sand (filling voids); inverse grading
GC III (115-160 cm)	Black (5Y 2.5/1) poorly sorted coarse to very coarse clast-supported pebbles; med. sand (filling voids); lenticular insets of coarse to very coarse sand and openwork granules/fine pebbles
GC IV (160-180 cm)	Black (5Y 2.5/2) discontinuous band of sandy loam wedges at level with adventitious tree roots on exhumed *in situ* stumps; coarse to very coarse pebbles of inverse grading to poorly sorted pebbly/granuly coarse sand.
GC V (180-265 cm)	Very dark olive to black (5Y 3/2, 5Y 2.5/2) massive poorly sorted clast-supported coarse pebbles to fine cobbles; coarse sand (filling voids); lenticular insets of angular openwork coarse to very coarse pebbles
GC VI (240-270 cm)	Discontinuous horizon of large, partly decomposed wood fragments topping a ~5 cm thick band of very dark olive to black (5Y 3/2, 5 Y 2.5/2) sandy clay loam
GC VII (270-305 cm)	Band of subrounded to rounded mod. well sorted clast-supported fine cobbles
GC VIII (305-320 cm)	Black (5Y 3/2.5Y 2.5/2) muscovite-rich mod. well sorted fine sand; slight bleaching and oxidation traces; charred tree rootlet
GC IX (? cm)	Poorly sorted pebbly/granuly coarse sand with some coarse pebbles

01/09/2001

Fig. 5. Typical stratigraphic section of fan terrace riser containing in situ tree trunks buried by landslide-induced aggradation at Gaunt Creek, Waitangitaona River, South Westland (X, Fig. 3). LWD=large woody debris in partly decomposed state; t=in situ tree. Coordinates refer to New Zealand Map Grid.

adjacent SH6 (Fig. 7). Several springs in the vicinity of the former channel course near the Waitangiroto River attest significant groundwater discharge (Fig. 3).

Cross-sections regularly carried out by Westland Regional Council, Greymouth, since 1982, were resurveyed to compute net aggradation rates and gradient changes on the fan (Fig. 8). Despite short-term

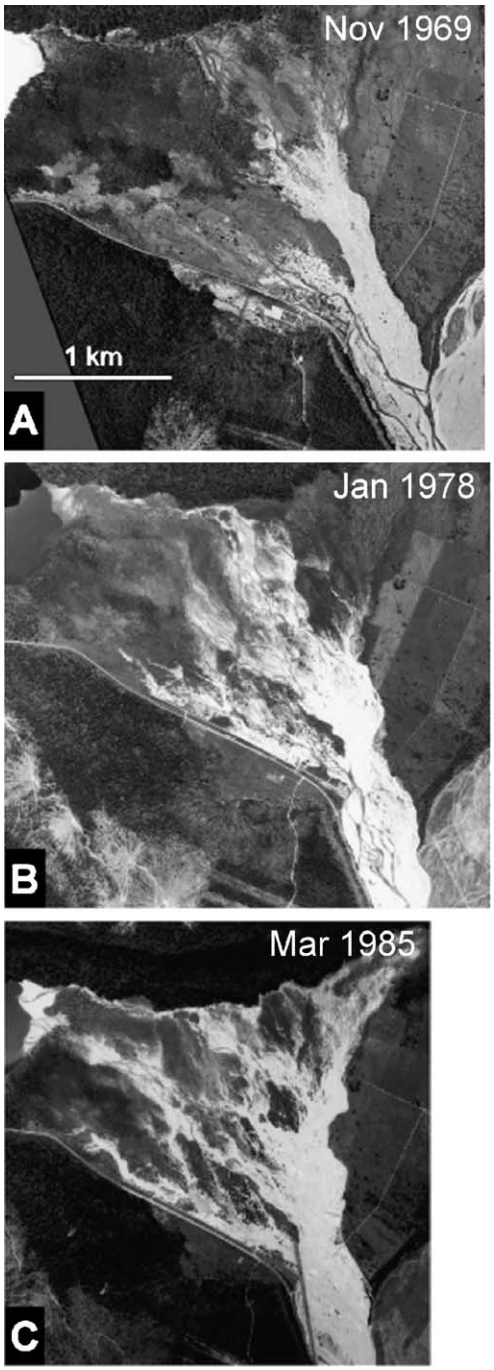

Fig. 6. Post-avulsion sequence of channel establishment of Waitangitaona River. Individual gravel lobes prograde over laterally unconfined and slightly convex fan surface covered by farmland and swamp forests. Images courtesy of Land Information New Zealand (A: SN4301/12; B: SN5188/G13; C: SN8493/E13, Crown©).

processes of frequent braid channel shift, the decade-scale changes in surface elevation reveal a complex pattern of net accretion and incision along the fan long profile (Fig. 8A). During the 1980s, an intersection point separated net fan-head trenching of 56 mm year^{-1} from distal deposition at >70 mm year^{-1}. Aggradation at the fan apex commenced again in the 1990s, while peak deposition (>80 mm year^{-1}) had shifted further downstream, possibly indicating a passing sediment wave. Distal fan portions were subject to continuous net deposition since at least 1982. The spatial variation in deposition is mirrored in the changing thalweg long profile (Fig. 8B). The straight long profile shown in 1982 markedly increased in curvature during the following two decades. Mean slope was reduced from 0.0085 to 0.0075 due to net incision of <2 m along the channel thalweg.

The fan-toe delta at Lake Wahapo is actively prograding, while only a small portion of undisturbed shoreline remains covered by stands of degraded kahikatea (*Dacrycarpus dacrydioides*) swamp forest. Incised delta channels respond to lake-level fluctuations and profile lengthening. The occurrence of coarse cobbles ($D_{max} \sim 180$ mm) in delta topsets attests an increase in transport capacity, when compared to the observations of Griffiths and McSaveney (1986), who reported fine pebbles with $D_{max} \sim 5$ mm as the maximum particle size in the mid-1980s.

5.2. Boulder Creek, Moeraki River

A similar avulsion sequence forced by tributary sediment input can be reconstructed for Boulder Creek on the lower Moeraki River (Fig. 1). Episodic debris slump and extremely rapid slide/flow in crushed hornfelsic sandstone and puggy tectonic breccia in the hill country NW of the Alpine Fault (Eggers, 1987) delivered debris to the steep ($\sim 13°$) debris fan of Boulder Creek. A total area of ~ 0.28 km^2 (18% of the fan) was affected by aggradation. The lower Moeraki River is occupying an infilled fjord, of which shallow Lake Moeraki and a low-gradient embayment valley-fill remain as a legacy. The input of landslide debris caused river metamorphosis (Schumm, 1969) with a nearly fourfold increase in active channel area immediately downstream of the confluence (Fig. 9), which gradually propagated

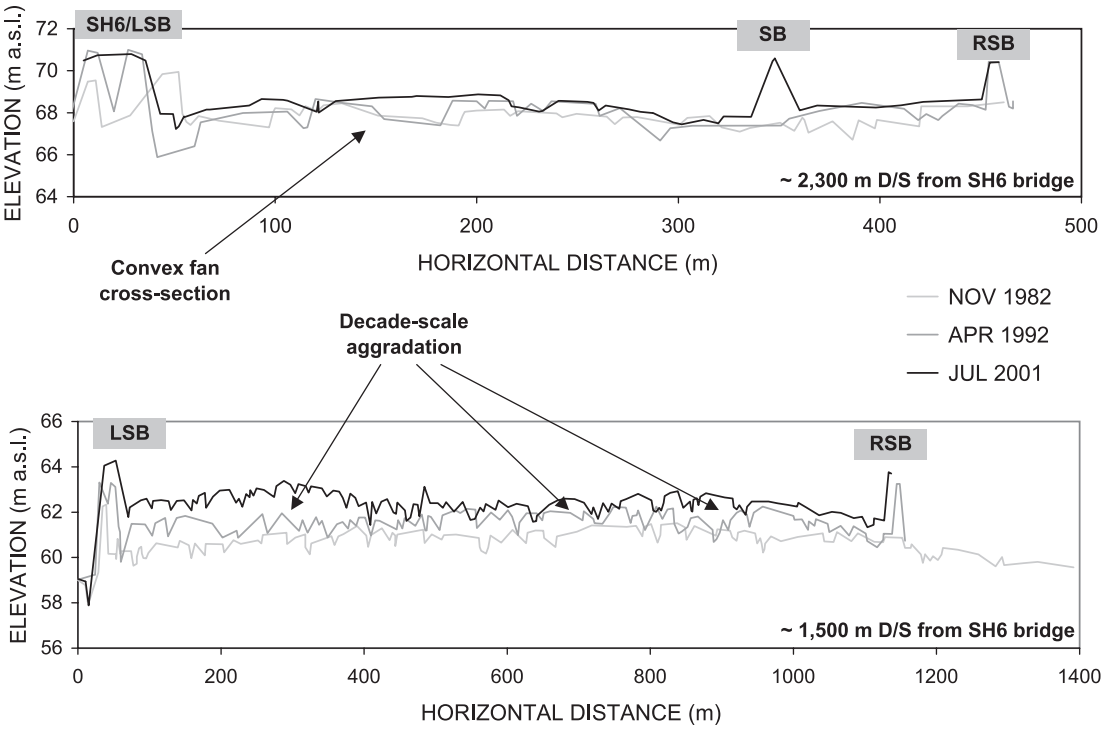

Fig. 7. Typical cross-sectional surveys of Waitangitaona River terminal fan. Fan morphodynamics are dominated by continuing net aggradation since the avulsion in 1967. SH6=State Highway 6; SB=stopbank; LSB=left stopbank; RSB=right stopbank.

downstream for nearly 2 km. Build-up of debris at the confluence caused a temporary occlusion of the Moeraki River channel, which has been partly preserved as a backwater pool.

Excessive in-channel aggradation promoted overbank deposition forming numerous coarse gravel splays, chutes, and floodouts (Figs. 4B and 10), while cut-off channel segments were sequentially reactivated or backfilled. Large areas of mature *Nothofagus* floodplain forest were buried by gravely sediment during multiple avulsions, suggesting a return period of >200–300 years for this event magnitude. Minimum burial depth along the affected reach ranges between 1.6 ± 0.2 m. The total post-1946 floodplain net deposition is estimated at $0.7\pm0.1\times10^6$ m^3 (Fig. 10), with minimum rates of floodplain accretion and incision of >45 mm year^{-1} since 1965.

These figures, however, include the upstream fluvial sediment yield and are not corrected for trapping efficiency of the lower Moeraki floodplain. The fragmented Moeraki River planform records previous occlusions by steep tributary debris fans similar to that of Boulder Creek, which have forced backstow of several swampy flats.

5.3. Mt. Adams rock avalanche, Poerua River

The 1999 Mt. Adams rock avalanche on the Poerua River is the most recent case of a landslide-induced channel avulsion in the study area (Fig. 1). Without any obvious trigger, $\sim10-15\times10^6$ m^3 of schistose bedrock and colluvium fell into the Poerua gorge and formed a 100-m-high landslide dam high (Hancox et al., 1999) about 3.5 km upstream of where the river debouches onto an alluvial fan at the mountain front (Fig. 11).

Overtopping of the landslide dam resulted in an outburst flood with a peak discharge of ~3000 m^3 s^{-1} and subsequent infilling of the gorge with landslide debris (Korup et al., in press). The sediment wave soon reached the alluvial fan. There, massive deposition caused a major channel avulsion,

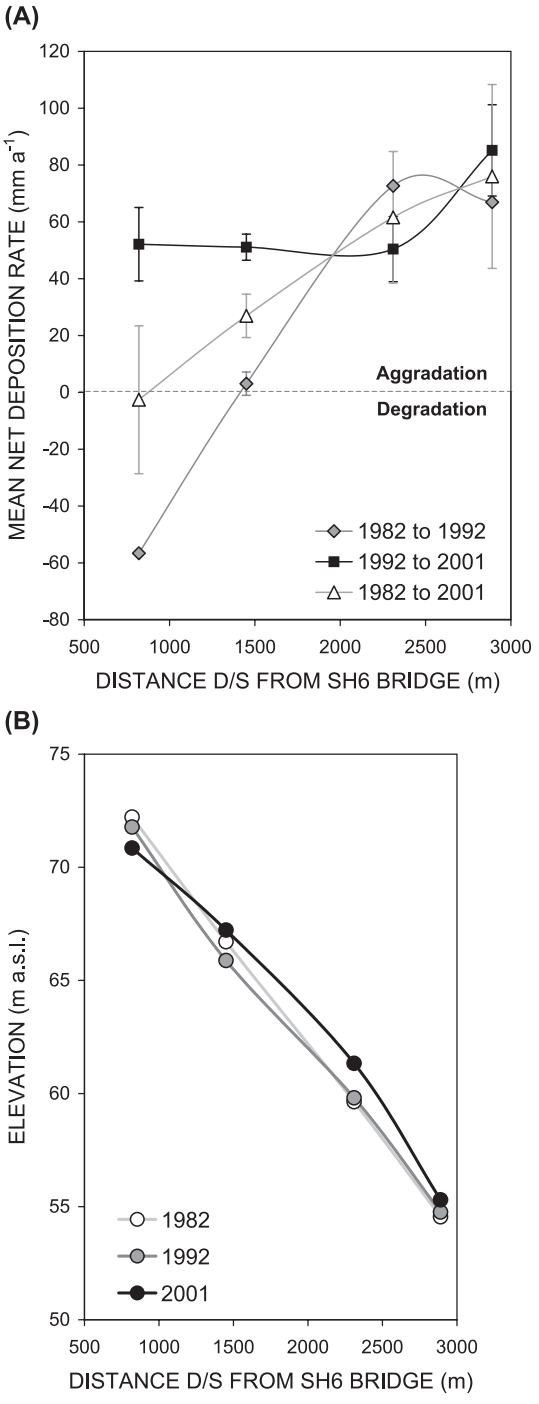

Fig. 8. (A) Mean net deposition rates on Waitangitaona River terminal fan from repeat surveys in between 1982 and 2001; (B) long profile along main thalweg from surveys conducted in 1982, 1992, and 2001.

which had reactivated a cut-off segment E of the original course of the Poerua River 16 months after the dam failure (Fig. 11). By early 2002, the avulsion channel had locally increased its active bed width by >200%, routing most of the discharge away from the former channel. The avulsion has so far destroyed ~0.9 km^2 of farmland by aggradation and fluvial scour. During a field visit in April 2002, the fan head was characterized by ongoing establishment of the avulsion channel traversing mature floodplain forest. Undergrowth was largely buried under >1 m thick sheets of sandy gravel as far as ~1.5 km downstream from the fan apex. Remnant patches of dense growth, large woody debris (LWD) jams, and log steps have forced numerous knickpoints and micro-cascades in laterally unstable and steep channel braids. Fan-head deposition and backfilling of the gorge is continuing and has buried former aggradation terraces, which had originally been ^{14}C-dated by Adams (1980), now yielding a re-calculated age of 295±55 BP (NZ 4630; D. Chambers, personal communication, 2002).

6. Regional analysis of landslide-induced channel avulsions

6.1. Regional pattern

Two of the three historic case examples of landslide-induced channel instability had major destructive impact on agricultural land and infrastructure, while the causative slope failures were located several kilometres upstream. In the study area, about 80% of all mapped landslides are coupled with the alpine trunk drainage network (defined as channel segments having a contributing catchment area A_c>10 km^2), with ~26% affecting areas >1 km^2. The length of the coupling interface between a landslide and the basal trunk channel is 1.2 km in average, and the length shows a power-law relationship with total affected landslide area A_m (Korup, 2003). Sixteen major channel avulsions on valley trains, intramontane alluvial flats, and mountain-fringe alluvial fans in the study area were selected for geomorphometric analysis (Fig. 1; Table 1). Evidence of additional smaller avulsions may well have been subject to obliteration by subsequent larger events or re-vegetation.

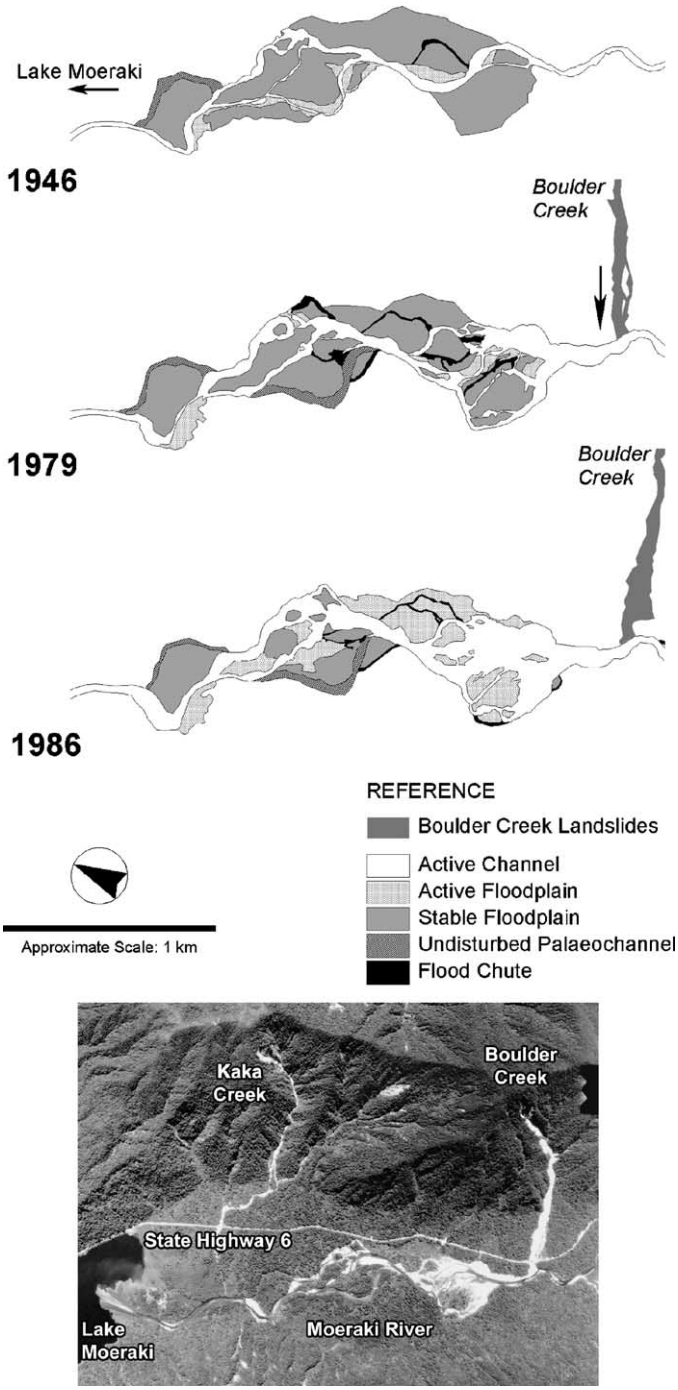

Fig. 9. Geomorphic sketch and air photo of landslide-induced avulsion on the lower Moeraki River, South Westland. Post-1946 slope instability in Boulder Creek caused excessive sediment input, gradual downstream increase of active channel/floodplain area, and avulsions due to reach-scale aggradation and associated reworking and/or burial of floodplain sections. Image courtesy of Land Information New Zealand (SNC8595/J14, Crown©).

Fig. 10. Massive in-channel aggradation on Boulder Creek at State Highway 6 bridge (March 2002). Overloading of channels by coarse landslide-derived sediment continues to be a problem to infrastructure long after the causative slope failure. River flow is from right to left.

Comparison of multi-temporal air photos depicts that all avulsions occurred as a consequence of debris input from nearby large landslides. Several geomorphometric parameters characterize the pre- and post-avulsion fluvial morphology (Table 1):

1. The total area affected by the avulsion (channel) A_n.
2. The maximum lateral displacement between the new and former channel courses L_{cs}.
3. The ratio $L_n L_f^{-1}$, i.e. the segment length ratio between the new and former channel courses.
4. The ratio of channel slope $S_n S_f^{-1}$ between the new and former channel courses.

At least 6% of all mapped landslides in the study area have caused large avulsions, which involved fluvial reworking of 0.6 ± 0.3 km^2 of floodplain or fan surfaces on average. Avulsion in total has affected nearly 34 km of channel length, while individual segments may be up to ~ 4 km long. Avulsed channels are slightly longer and $\sim 20\%$ steeper than abandoned channel segments on average (Table 1). Relative channel lengthening occurred where avulsion channels had established around a landslide or debris-fan toe. The mean lateral channel shift is ~ 750 m and highest on unconfined alluvial fans. The three case histories show that alluvial fans create ideal conditions for avulsions on major rivers draining steep alpine catchments prone to frequent rainfall- and earthquake-triggered landslides (Yetton et al., 1998). To test the hypothesis whether landslide-induced river channel avulsions result from the exceedance of a critical ratio between landslide and catchment size, potential influences of geomorphometric scaling relationships and sediment input were examined more closely.

6.2. Scaling relationships

Total affected (planform) area A_m is a common measure for landslide "magnitude" and determined by mapping. Contributing catchment area A_c derived from the DEM is used as a proxy for discharge, and thus fluvial "removal power". Regional flood frequency attests a low flood variability for rivers in the study area, where the 0.01 annual exceedance probability flood discharge is only twice that of the mean annual flood (McKerchar and Pearson, 1989). Mean relative errors of $\pm 30\%$ in A_m (Korup, 2003) favoured a first-order graphical analysis of the relationship between A_m and A_c over more robust statistical methods. Therefore, a sample of n=135 landslide-affected river reaches was compiled from multi-temporal air photos. Reaches were treated as landslide-affected, where they exhibited an assemblage of landslide scars and deposits (A_m roughly $>10^5$ m^2),

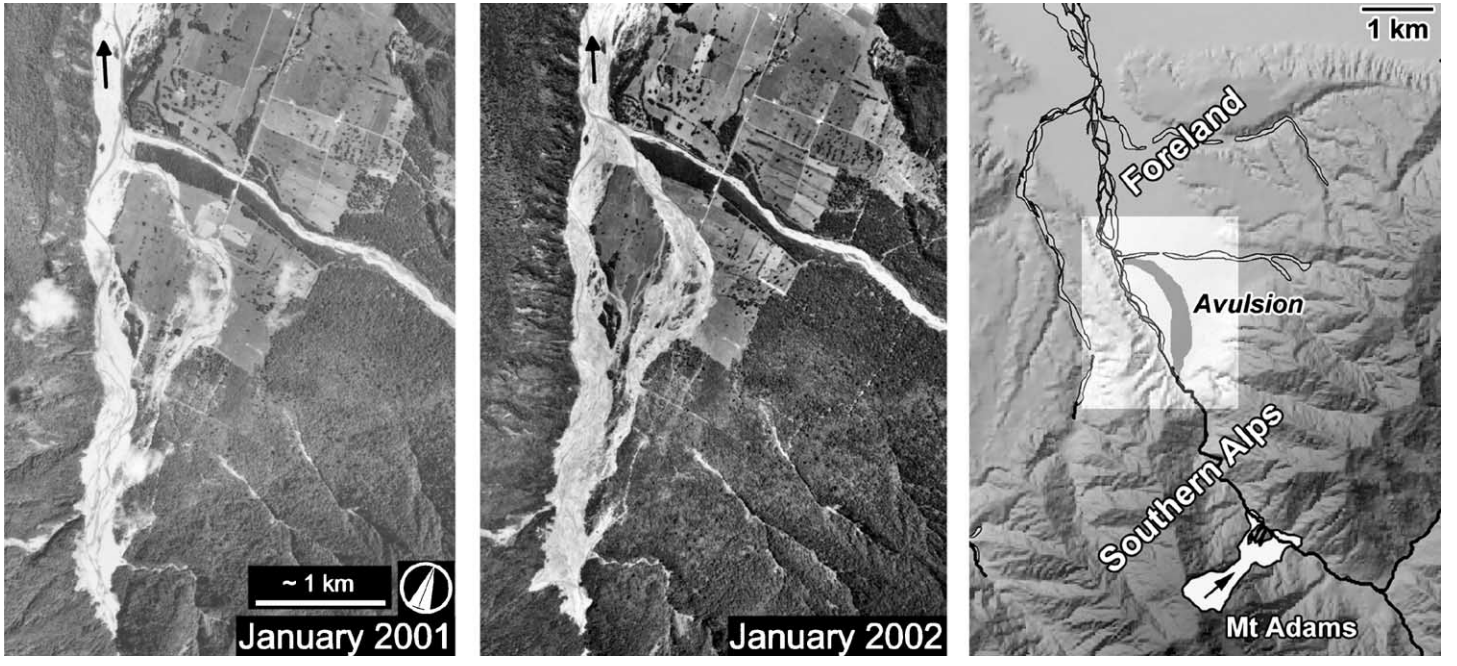

Fig. 11. Sequential air photos of landslide-induced avulsion, Poerua River, following the failure of a rock-avalanche dam in 1999. Incipient downstream aggradation and avulsion is evident in January 2001, ~6 months after the event. Establishment of the avulsion channel course is nearly complete after ~30 months. Note tributary fan-toe trimming and minor flood chute formation. Images courtesy of Department of Natural Resources and Engineering, Lincoln University (SN12690B/A6, SN12690B/A08).

Table 1
Geomorphometric characteristics of selected landslide-induced river channel avulsions in mountain catchments of South Westland and northern Fiordland

River	Avulsion area A_n (km^2)	Avulsion length L_n (km)	Length ratio L_n/L_f	Slope ratio S_n/S_f	Lateral displacement L_{cs} (km)	Date of formation	Type[a]	New Zealand Map Grid[b]	
								E	N
Waitaha	n/a	2.7	n/a	n/a	n/a	1900s	C	2325240	5786600
Poerua	0.8	3.3	1.08	1.22	0.7	2000	D/S	2308920	5773750
Waitangitaona	3.7	4.0	n/a	n/a	3.2	1967	D/S	2291480	5765830
Karangarua (Misty Peak)	n/a	4.3	1.43	n/a	0.7	prehistoric	C	2253890	5724920
Karangarua (Cassel Flat)	n/a	0.7	0.68	n/a	0.25	n/a	U/S	2254420	5722390
Manakaiaua	0.6	1.8	0.95	1.06	0.65	n/a	D/S	2245370	5732560
Hall	0.04	1.2	1.11	n/a	0.3	historic	C	2222620	5716860
Paringa/Otoko	0.1	2.5	1.20	n/a	1.04	n/a	D/S?	2229470	5708310
Moeraki (Boulder Creek)	0.5	2.0	0.79	1.27	0.45	post-1946	D/S	2214110	5709520
Moeraki (Horseshoe Flat)	0.03	0.8	0.63	1.60	0.62	prehistoric	U/S	2218890	5704710
Waiatoto (Charlie's Ponds)	0.2	1.4	1.43	n/a	0.6	n/a	C	2173960	5665930
Cascade (D/S Falls Creek)	0.3	2.9	0.99	1.12	0.8	?	C	2144640	5653970
Pyke	0.2	2.4	0.86	1.16	1.08	n/a	U/S	2127570	5625840
Tutoko (Leader Flat)	0.4	2.1	1.07	1.02	0.47	n/a	D/S	2112750	5607290
Clinton (West Branch)	0.05	0.7	1.45	n/a	0.34	1982	C	2103490	5579880
Camelot	n/a	0.9	1.22	n/a	0.37	n/a	C	2054770	5528300
MEAN	**0.58**	**2.1**	**1.06**	**1.21**	**0.77**	–	–	–	–

[a] D/S=downstream or loading avulsion; U/S=upstream or backwater avulsion; C=contact avulsion (see text for explanation).
[b] Divergence point.

together with discernible changes to channel geomorphology in the landslide vicinity as opposed to adjacent reaches. The sample was stratified by the dominant direction of fluvial response inferred: aggradation up- or downstream of the landslide, active blockage, or channel re-routing around the landslide deposit (occlusion). The resulting plot shows homogeneous scatter (Fig. 12), indicating that river-disturbing landslides of mostly all sizes may occur anywhere from headwaters to downstream reaches.

The majority (~46%) of river-impacting landslides affect an area ~1–10% that of the upstream catchment area. Nearly 53% involve lateral occlusion, ~25% upstream effects such as blockage or aggradation, and ~19% dominantly downstream aggradation. Nonetheless, the scaling relationship between landslide and catchment size is inadequate for discriminating the principal direction of fluvial response from, for example, distinct clusters or envelope curves. Similar approaches used in studies on landslide dams showed that the vertical dimension, such as the mean or maximum thickness of landslide deposits emplaced in river channels or valley floors, may yield better graphical separation of the basic type of fluvial response (Korup, 2003).

6.3. Landslide-derived sediment input

Excessive lateral sediment input is a critical control on fluvial transport capacity and morphology. The case examples demonstrate that overloading of river channels causes aggradation, reduction of channel cross-sectional area, and lateral instability. Recent sediment budgets of debris input by large historic

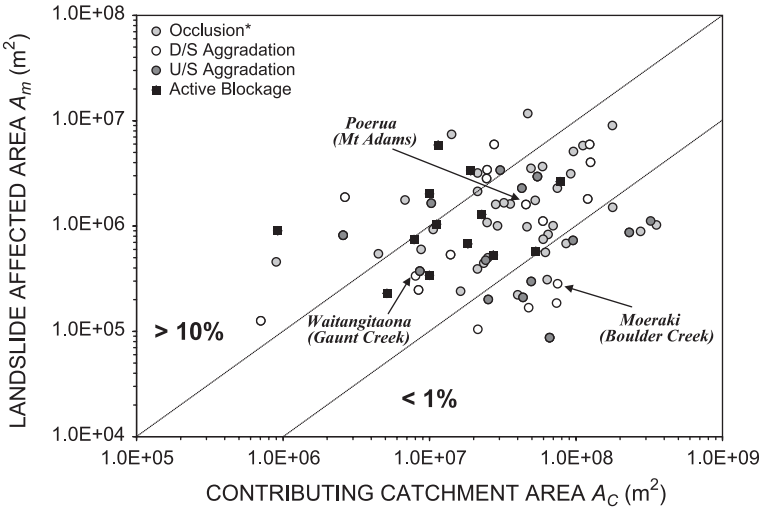

Fig. 12. Scaling relationship between landslide (planform) area A_m and contributing catchment area A_c for a sample of n=135 landslide-impacted river reaches in the study area. Data are stratified by observed dominant fluvial response (*occlusion includes on-site channel changes such as, e.g. diversion of flow around landslide toes) as inferred from multi-temporal air photos, geomorphic evidence, and ground truthing. The high scatter does not permit any discrimination of fluvial response on the basis of planform characteristics.

landslides (Korup et al., in press), however, found the contribution from discrete sources difficult to distinguish from the overall sediment yield. Mean long-term estimates of sediment discharge from, for example, large rock avalanches in the Southern Alps (Whitehouse, 1983) correlate only moderately with landslide volume, showing order-of-magnitude variation for a given landslide volume (r=0.57, S.E.=48%). Although estimated long-term (10^3 year) rates may attain >80,000 m^3 year^{-1}, they are surpassed by historic rates by an order of magnitude. Comparison with sediment discharge derived from a regional 40-year landslide inventory (Hovius et al., 1997), short-term gauge measurements (Griffiths, 1981) and sediment budgets (Korup et al., in press) shows substantial scatter in historic delivery rates of landslide debris (Fig. 13).

Depending on the length of the observation period, averaged historic sediment discharge may vary by >300%. Even the estimated maximum sediment discharge on the Waitangitaona River is markedly lower than the regional trend in catchments devoid of any major historic landslide disturbance (Fig. 13). The main problem of sediment budgets with respect to short-term gauging data is the unknown quantity of suspended sediment load, which has escaped deposition. Thus, while indicating very high process dynamics, these sediment budgets are also fraught with inevitable problems of accuracy and unspecified variability in alpine sediment flux. Given such constraints, a sediment budget approach is deemed inappropriate for delineating critical thresholds of sediment input to trigger large-scale aggradation and avulsion in the study area.

6.4. Fluvial response and recovery

The fluvial response times for avulsion to occur following landslide disturbance varied amongst the case examples, but were generally <30 years. Recurrence intervals of landslide-driven avulsion at-a-site are estimated to be in the order of 10^2 years, based on ^{14}C dates combined with tree-ring and gird-width measurements of excavated in situ trees (Fig. 2F). The magnitude of historic aggradation at Gaunt Creek has been the largest in ~200–300 years, and historic air photos show that Gaunt Creek Slip has been the largest active slope failure in the Waitangitoana River catchment during the 20th century. To assess the rapidity of fluvial recovery, process rates of historic landslide-induced avulsions are compared with long-term trends. Local degradation rates over 10^2–10^3

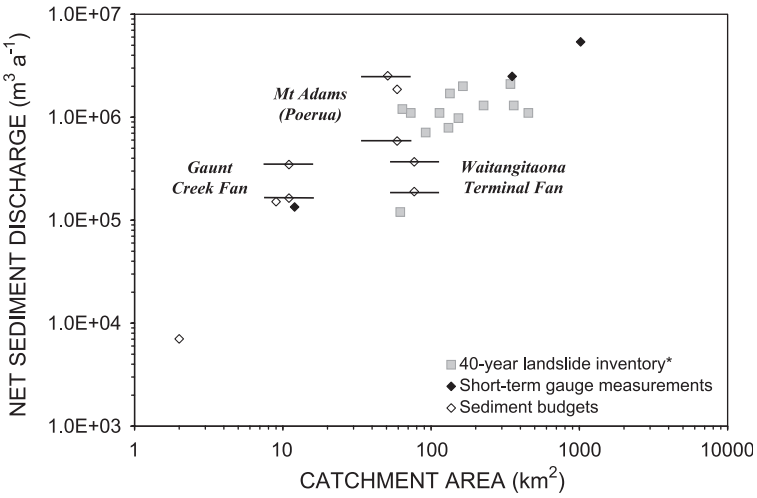

Fig. 13. Net sediment discharge from alpine catchments in South Westland plotted against contributing catchment area (treated as a proxy for discharge). Data comprise extrapolations from a ~40-year landslide inventory (*Hovius et al., 1997), short-term gauge measurements (Griffiths, 1981), and estimates from sediment budgets based on geomorphic evidence (Korup et al., in press). Horizontal bars denote estimated range of sediment discharge from historic landslides discussed in the text.

years can be estimated from compiled field data by dividing the thickness of discrete fluvial deposits by their absolute (^{14}C-)age inferred from, for example, buried soils or large wood fragments (Table 2).

Man-made relics may also be very valuable in recording medium-term fluvial change. For example, groynes on Pegleg Flat, the Otira River in central Westland, dating to ~1923, when the first railway tunnel to reach the western Southern Alps had been constructed, were found stranded on a ~10-m-high terrace above the present river bed. The inferred degradation rates of 107±36 mm year^{-1} during the 20th century are substantial. Nonetheless, mean long-term incision rates plotted against contributing catchment areas vary by two orders of magnitude for a given catchment area, allowing for a ±30% error range for potential inaccuracy in terrace height measurements (Fig. 14A).

This poor correlation can be explained by the very high process rates associated with historic avulsions, which are less prone to stratigraphic censoring effects of the long-term fluvial record (Kirchner et al., 2001). In fact, the inferred mean degradation rates appear to decrease as a function of the age assigned to the respective markers in a moderate self-similar fashion (Fig. 14B). The rapidity of decadal-scale aggradation, avulsion, and recovery by subsequent degradation, however, bear high hazard implications for river engineering and land use management.

7. Discussion: a typology of landslide-induced river channel avulsions

This study presents the first comprehensive collection of data and observations pertaining to landslide-induced river channel avulsions in New Zealand. Fluvial process rates or data on magnitude and frequency of avulsions are of high importance in catchment management. Furthermore, critical thresholds separating reversible from irreversible impacts should be ideal determinants of catchment sensitivity to landslide impact (Downes and Gregory, 1993; Brunsden, 2001). However, geomorphometric analysis has shown that neither a scaling relationship between landslide and catchment size nor quantification of sediment input are adequate to delineate such thresholds. This problem arises not so much from the lack of any empirical or physical explanations. The high morphodynamic variability in tectonically active mountain belts rather imposes inevitable limitations to accurate sampling of geomorphometric and process data on landslides and

Table 2
Approximate mean degradation rates of several Westland rivers inferred by ^{14}C dates and other dating methods (compiled from several sources)

River (location)	Dated landform	Dating method[a]	Age[a] (years)	Deposit thickness (m)	U/S catchment area (km^2)	Mean degradation rate (mm year^{-1})		New Zealand Map Grid		Reference
						Min	Max	E	N	
Otira (Pegleg Flat)	Historic groynes stranded on true right terrace	Estimate	72	5–10	13.1	71	143	2392215	5811655	This study
Karangarua (McTaggart Ck)	Re-exhumed in situ tree stumps in present river bed at McTaggart Ck confluence	^{14}C (NZ 1292; Wk 5264)	*362±84; 420±25*	15–30	171.8	26	87	2253820	5726435	D. Chambers (personal communication, 2002), Yetton et al. (1998)
Copland (Welcome Flat)	Re-exhumed trees in situ on true left present river bank	^{14}C (NZ 1293)	*1527±73*	5–10	64.5	3	7	2265980	5725425	D. Chambers (personal communication, 2002), Adams (1980)
Paringa I (Alpine Fault)	In situ tree stumps in carbonaceous layers of Paringa Formation	^{14}C (Wk 2322)	3670±40	3–5	222.6	1	1	2228000	5714700	Simpson et al. (1994)
Paringa II (Alpine Fault)	In situ tree stumps in carbonaceous layers of Paringa Formation	^{14}C (Wk 2321)	9630±70	14–16	223.0	1	2	2228000	5714700	Simpson et al. (1994)
Paringa III (Alpine Fault)	Fossiliferous laminated silts containing angular schist fragments	^{14}C (NZ 531)	13,790±150	62–77	222.6	4	6	2227900	5714800	Simpson et al. (1994)
Wanganui (U/S of AlpineFault)	Wood derived from 12-m terrace at 8 m above river level; estimated 80 years of missing tree rings	^{14}C (NZ 4628)	*504±56*	8	264.8	14	14	2321000	5776300	D. Chambers (personal communication, 2002), Adams (1980)
Waitangitaona (SH6)	Terminal fan head of Waitangitaona River, ~800 m D/S of SH6 bridge	Repeat Survey	10	0.5	77.0	56	57	2292030	5766080	This study

Poerua I (Alpine Fault)	Wood from 10-m aggradation terrace	^{14}C (NZ 4630)	*295±55*	8–10	59.7	17	29	2309000	5777380	D. Chambers (personal communication, 2002), Adams (1980)
Poerua III (Alpine Fault)	Sapwood from rata branch in aggradation terrace 1 km D/S of Alpine Fault	^{14}C (Wk 4340)	370±60	6	65.3	11	13	2308300	5774700	Yetton et al. (1998)
Gaunt Creek (Alpine Fault)	Multiple historic aggradation terraces	Survey	>36	5.3	10.2	147	217	2292250	5762620	This study
Haupiri (Crane Ck)	Beech log from aggradation terrace	^{14}C (Wk 4343)	390±50	4	9.1	7	8	2409800	5846500	Yetton et al. (1998)
Hokitika I (Muriel Ck)	Sapwood from ribbonwood branch in 4-m aggradation terrace, 400 m U/S of Alpine Fault	^{14}C (Wk 4439)	540±60	4	7.5	6	7	2350200	5803200	Yetton et al. (1998)
Hokitika II (Muriel Ck)	6-m aggradation terrace, 400 m U/S of Alpine Fault	^{14}C (Wk 4339)	810±60	6	7.5	7	8	2350200	5803200	Yetton et al. (1998)
Cascade (Mt. Delta)	Beech log from 3-m terrace in rockfall-derived breccia on true left of present river bed	^{14}C (NZ 4624)	*1572±60*	3	231.1	2	2	2150800	5663500	D. Chambers (personal communication, 2002)
Kokatahi (Alpine Fault)	Twigs from top of 5-m aggradation terrace	^{14}C (Wk 4009)	330±60	5	100.4	10	14	2357900	5810300	Yetton et al. (1998)
Toaroha I (Alpine Fault)	Kamahi log in base of aggradation terrace on true left	^{14}C (Wk 4019)	650±60	3	67.3	4	5	2357200	5809900	Yetton et al. (1998)
Toaroha II (Alpine Fault)	Rata log in same terrace as above, but on true right	^{14}C (Wk 4013)	580±60	2.7	67.6	4	5	2357300	5810200	Yetton et al. (1998)
Styx (Alpine Fault)	Rata branch from 2-m aggradation terrace	^{14}C (Wk 4011)	680±50	2	55.6	3	3	2359500	5812200	Yetton et al. (1998)
Haupiri (Alpine Fault)	Beech log from aggradation terrace 200 m U/S of Alpine Fault	^{14}C (Wk 4874)	260±50	3	91.1	6	9	2405600	5843700	Yetton et al. (1998)

[a] Including laboratory sample numbers for ^{14}C dates; calibrated and re-calculated ^{14}C ages are indicated in italics.

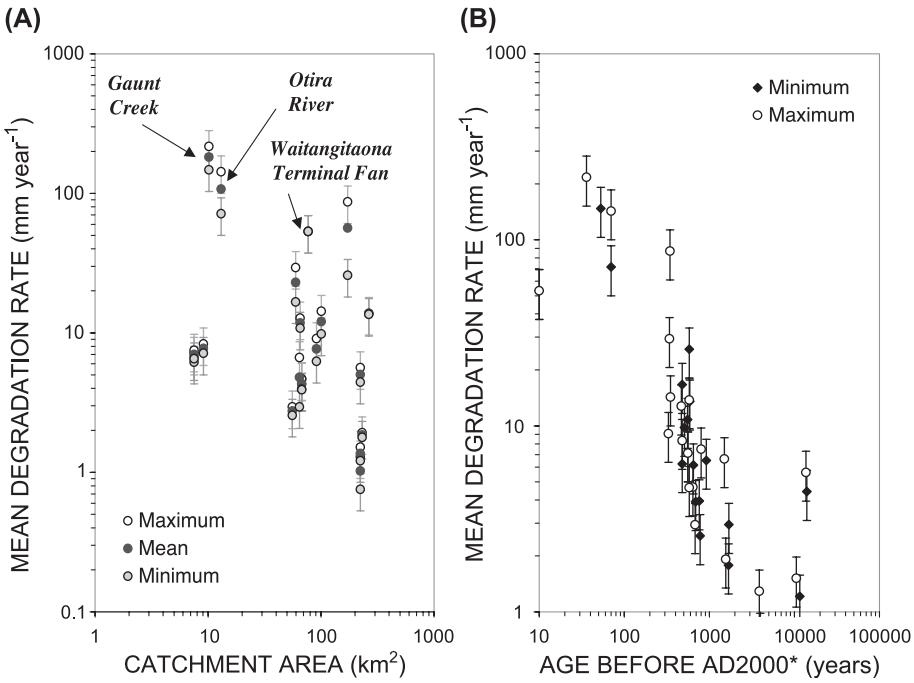

Fig. 14. Mean long-term degradation rates from dated aggradation terraces in selected Westland rivers (cf. Table 2) versus (A) contributing catchment area. Error bars allow for ±30% inaccuracy of terrace heights; (B) terrace age (*approximate only due to several non-calibrated ^{14}C dates involved). Rates indicate moderate self-similarity over three orders of magnitude despite possible effects of local uplift rates or age-related censoring in the morphostratigraphic record.

rivers. Data frequently scatter on an order-of-magnitude scale and meaningful comparisons should consequently employ this fact. To overcome these problems and to typify landslide-induced river channel avulsions, the basic principles of Figs. 12–14 were augmented with interpretations of geomorphic process response of rivers to landslide impact from sequential air photos (Korup, 2003). The resulting nominal classification recognizes the principal direction of fluvial response with respect to its position relative to the emplacement site of the disturbing landslide deposit. It is also implicitly based on the combined influence of scaling relationships, sediment discharge, and fluvial recovery (Fig. 15).

7.1. Upstream or backwater avulsions

The principal trigger for upstream or backwater channel avulsion is a prolonged backwater effect induced by full blockage, which was recorded at 25% of the 135 investigated landslide-impacted river reaches (Fig. 15A,B). Landslide-damming forces a rise of local base-level and reduces reach-scale gradient, stream power, and fluvial transport capacity, while backwater aggradation commences infilling of the landslide-dammed lake via prograding gravel fan-deltas. In the study area, at least three major backwater avulsions (Table 1) have occurred due to lake-level fluctuations, fan-delta growth, or gradual profile lengthening (Jones and Schumm, 1999). By definition, the occurrence of this avulsion type is dependent on the stability of the landslide barrier. Korup (2003) showed that in New Zealand dam heights >10% of the upstream catchment relief are a characteristic of existing landslide dams.

7.2. Contact avulsions

Contact avulsions are the most common type in the study area (53%) and occur on-site due to physical landslide impact and subsequent channel re-establishment along an altered, usually perched,

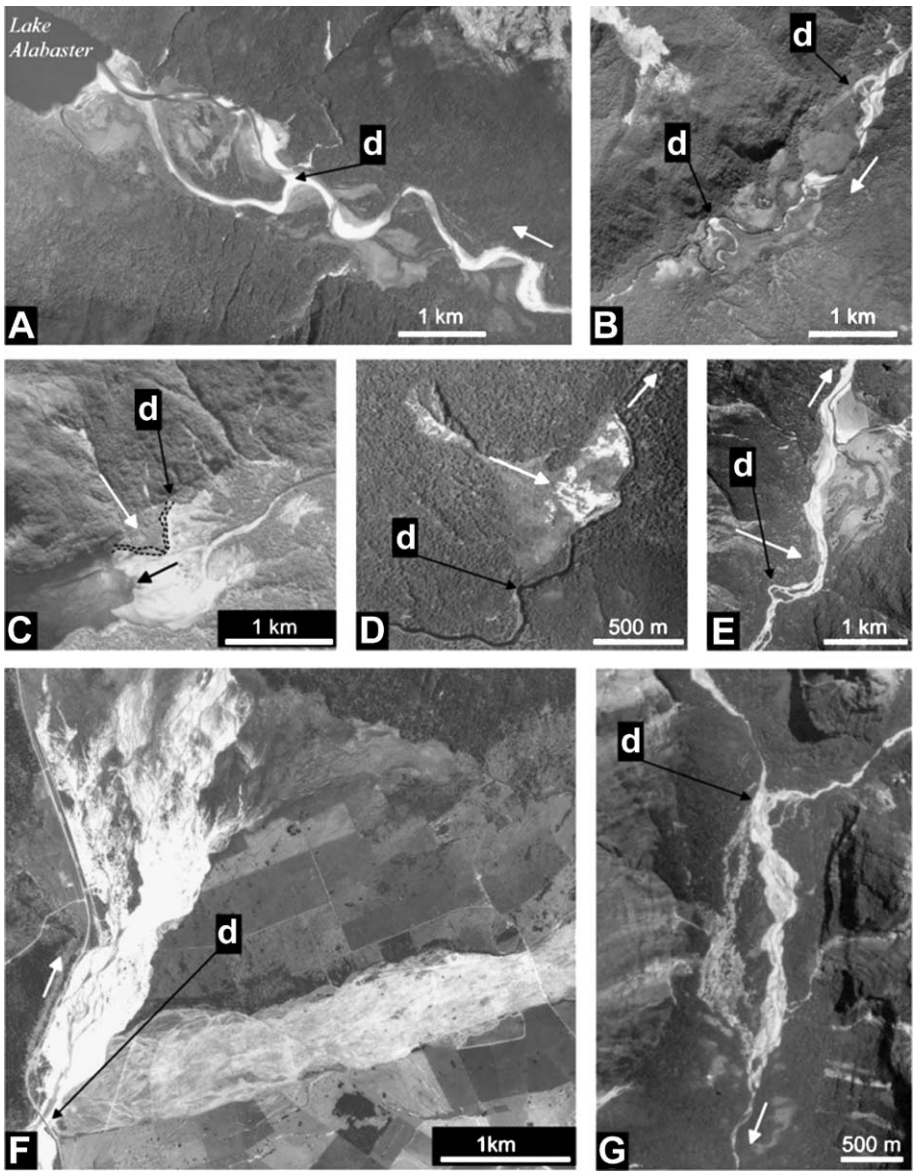

Fig. 15. Types of landslide-induced channel avulsions in SW New Zealand; d=divergence point. (A) Backwater avulsion upstream of Lake Alabaster, Pyke River (SN8426/D7); (B) backwater avulsion on Horseshoe Flat, Moeraki River (SN5941/D22); (C) contact avulsion at debris-fan toe, Camelot River mouth, Broadshaw Sound (SN9066/E10); (D) partial contact avulsion, Hall River (SN5941/B27); (E) contact avulsion upstream of Axius Flat, Waiatoto River (SN9065/B11); (F) loading avulsion on mountain-front fan of the Waitangitaona River (SN5188/G13); (G) loading avulsion on Tutoko River (SN8996/B6). All images courtesy of Land Information New Zealand (image numbers as indicated, Crown©).

course around or across the debris. In the case of deep-seated base failures, thrust or heave processes at the landslide toe actively cause vertical channel displacement, thus not necessarily causing length or slope shortening (Table 1). Post-impact channel adjustment occurs through either seepage, overtopping, bypass of the landslide debris, or a combination of these processes. Breach or spillway planform is

influenced by the deposit surface geomorphometry, roughness, armouring, and valley constriction. Seepage through unconsolidated landslide debris reduces surface discharge and decelerates channel re-establishment. Contact avulsions often form conspicuous low-wavelength incision meanders on distal landslide deposits (Fig. 15D), which are morphogenetically related to landslide-dam spillway channels, epigenetic gorges (Hewitt, 1998), and channel occlusions by debris-flow fans (Fig. 15C–E).

7.3. Downstream or loading avulsions

About 19% of landslide-impacted river reaches were dominated by downstream aggradation in the form of sediment waves derived from landslide debris (Sutherland et al., 2002; Clague et al., 2003). Downstream or loading avulsions result from the progressive loss of cross-sectional channel capacity causing increased flood frequency and overbank deposition of gravel lobes on valley trains or alluvial fans (Fig. 15F,G). In contrast to the other types of landslide-induced channel avulsions, the loading type is a direct result of increased sediment transport rather than physical channel blockage, occlusion, or diversion. The three case histories presented belong to this type, and have occurred on large unconfined alluvial fans. This explains their relative dominance in terms of mean total affected area (~ 1 km^2), avulsion channel length (~ 2.6 km), and lateral displacement (~ 1.1 km). The preferential re-occupation of former channel courses, such as cut-off meanders, chute scars, or former avulsion traces is a significant characteristic of loading avulsions. Although limited, such first-order predictability on the basis of local channel bank morphology (Field, 2001) renders detailed mapping of former channel courses an important contribution to avulsion hazard assessment for settlements, land use, and infrastructure on floodplains and alluvial fans (Zarn and Davies, 1994). Numerous former channel courses are readily identifiable on air photos; mapping their planform, capacity, and susceptibility to flood routing is recommended as an integral part of natural hazard mitigation in the region. The lower Makawhio (Jacobs) River, South Westland, exemplifies the potential of future aggradation-induced channel changes along well-defined traces of former avulsion or lateral channel migration (Figs. 1 and 16).

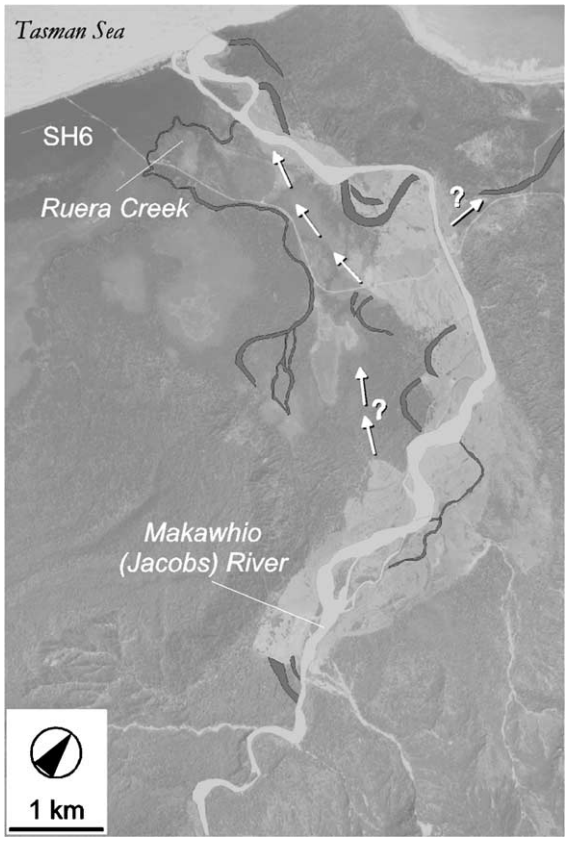

Fig. 16. Low-contrast air photo showing traces of former channel avulsions and lateral migration (dark grey) on the lower Makawhio (Jacobs) River, South Westland. The foothills of the Southern Alps are visible E of the farmed floodplain. Re-occupation of former channel courses may control future avulsions in the wake of extensive landslide-induced aggradation (white arrows); SH6=State Highway 6. Image courtesy of Land Information New Zealand (SN5188/D4, Crown©).

In contrast, channel patterns on active braidplains in the South Westland piedmont host few sensitive indications of discrete aggradation pulses. Only in limited cases are sequential air photos useful for analysing historic aggradation, such as on the proglacial Waiho River fan (Davies and McSaveney, 2000).

8. Conclusions

Geomorphic and air photo evidence of (pre-)historic landslide-induced channel avulsions was analysed in the mountainous SW of New Zealand. It

shows that landslides can alter on- and off-site channel morphodynamics and sediment discharge of mountain rivers to the degree of large-scale avulsion and river metamorphosis (Schumm, 1969). The lack of conclusive trends in quantitative data on geomorphometric scaling relationships and landslide-derived sediment discharge has necessitated a qualitative approach to classify avulsion types. This recognises the dominant direction of fluvial response with regard to the landslide emplacement site, and comprises upstream/backwater, contact, and downstream/loading avulsions. Only loading avulsions in the wake of high sediment input are independent of any direct physical contact with or blockage by landslide debris.

The unconfined alluvial fans at the South Westland mountain range front favour large-scale loading avulsions with high hazard implications. In a regional neotectonic context, the historic events on the Waitangitaona, Moeraki, and Poerua Rivers are important examples of aggradation and avulsion sequences caused by aseismic landslides. Process response may be similar in the wake of large-magnitude earthquakes on the Alpine Fault (Yetton et al., 1998), and care must be taken when interpreting the morphostratigraphic record of prehistoric events. Fluvial response to landslide-driven aggradation is rapid on decadal scales and exceeds long-term trends on an order-of-magnitude scale (Kirchner et al., 2001). This finding has important implications for post-earthquake landscape dynamics and future studies on the recent fluvial stratigraphic record in the region.

Several of the observed loading avulsions had reoccupied former channel courses (“second-order avulsion” of Nanson and Knighton, 1996). Further research on landslide-driven river disturbance will have to elucidate whether and on what time scales terms such as “robust” or “responsive” (Werritty and Leys, 2001) may be applied to the rivers in the region.

Acknowledgements

The author would like to thank Mike Shearer, West Coast Regional Council, Greymouth, for survey data on the Waitangitaona River. Dawn Chambers, Institute for Geological and Nuclear Sciences, Lower Hutt, kindly provided re-calculated several ^{14}C dates, and Sandy Brand, Department of Conservation, Te Anau, made data available for the Fiordland region. Timothy R. Davies, Department of Natural Resources and Engineering, Lincoln University, Canterbury, supplied air photos of the Poerua River. The constructive comments of Gary Brierley, Futoshi Nakamura, and Takashi Oguchi greatly helped to improve an earlier manuscript.

References

Adams, J., 1980. Palaeoseismicity of the Alpine fault seismic gap, New Zealand. Geology 8, 72–76.

Anthony, E.J., Julian, M., 1999. Source-to-sink sediment transfers, environmental engineering and hazard mitigation in the steep Var River catchment, French Riviera, southeastern France. Geomorphology 31, 337–354.

Bartarya, S.K., Sah, M.P., 1995. Landslide induced river bed uplift in the Tal Valley of Garhwal Himalaya, India. Geomorphology 12, 109–121.

Brunsden, D., 2001. A critical assessment of the sensitivity concept in geomorphology. Catena 42, 99–123.

Clague, J.J., Turner, R.W., Reyes, A.V., 2003. Record of recent channel instability, Cheakamus Valley, British Columbia. Geomorphology 53, 317–332.

Cooper, A.F., Norris, R.J., 1994. Anatomy, structural evolution, and slip rate of a plate-boundary thrust: the Alpine Fault at Gaunt Creek, Westland, New Zealand. Geological Society of America Bulletin 106, 627–633.

Craw, D., Youngson, J.H., Koons, P.O., 1999. Gold dispersal and placer formation in an active oblique collisional mountain belt, Southern Alps, New Zealand. Economic Geology 94, 605–614.

Davies, T.R., McSaveney, M.J., 2000. Anthropogenic fanhead aggradation, Waiho River, Westland, New Zealand. In: Mosley, M.P. (Ed.), Gravel-bed Rivers. V: Proceedings of Gravel-Bed Rivers 2000, 27 August–2 September 2000, Water Resources Publication, LLC., Christchurch, pp. 531–553.

Downes, P.W., Gregory, K.J., 1993. The sensitivity of river channels in the landscape system. In: Thomas, D.S.G., Allison, R.J. (Eds.), Landscape Sensitivity. Wiley, Chichester, pp. 15–30.

Eggers, M.J., 1987. Engineering geology assessment of slope instability on forest lands in South Westland. Unpublished MSc thesis, University of Canterbury, Christchurch, 345 pp.

Field, J., 2001. Channel avulsion on alluvial fans in southern Arizona. Geomorphology 37, 93–104.

Goedhart, M.L., Smith, N.D., 1998. Braided stream aggradation on an alluvial fan margin: Emerald Lake fan, British Columbia. Canadian Journal of Earth Sciences 35, 534–545.

Griffiths, G.A., 1981. Some suspended sediment yields from South Island catchments, New Zealand. Water Resources Bulletin 17, 662–671.

Griffiths, G.A., McSaveney, M.J., 1986. Sedimentation and river containment on Waitangitaona alluvial fan—South Westland, New Zealand. Zeitschrift für Geomorphologie 30, 215–230.

Hancox, G.T., McSaveney, M.J., Davies, T.R., Hodgson, K., 1999. Mt. Adams rock avalanche of 6 October 1999 and subsequent formation and breaching of a large landslide dam in Poerua River, Westland, New Zealand. Institute Of Geological & Nuclear Sciences Science Report 99/19 (Lower Hutt, 22 pp.).

Heim, A., 1932. Bergsturz und Menschenleben. Beiblatt zur Vierteljahresschrift der Naturforschenden Gesellschaft Zürich 20 (217 pp.).

Henderson, R.D., Thompson, S.M., 1999. Extreme rainfalls in the Southern Alps of New Zealand. Journal of Hydrology. New Zealand 38, 309–330.

Hewitt, K., 1998. Catastrophic landslides and their effects on the Upper Indus streams, Karakoram Himalaya, northern Pakistan. Geomorphology 26, 47–80.

Hicks, D.M., Hill, J., Shankar, U., 1996. Variation of suspended sediment yields around New Zealand: the relative importance of rainfall and geology. In: Walling, D.E., Web, B.W., (Eds.), Erosion and Sediment Yield: Global and regional perspectives, vol. 236. IAHS Publication, pp. 149–156.

Hovius, N., Stark, C.P., Allen, P.A., 1997. Sediment flux from a mountain belt derived from landslide mapping. Geology 25, 231–234.

ICIMOD (International Centre for Integrated Mountain Development), 2000. Mountain flash floods. http://www.icimod.org/publications/newsletter/New38/n38toc.htm.

Jones, L.S., Schumm, S.A., 1999. Causes of avulsion: an overview. In: Smith, N.D., Rogers, J. (Eds.), Fluvial Sedimentology. VI: International Association of Sedimentologists Special Publication, vol. 28. Blackwell, Oxford, pp. 171–178.

Kirchner, J.W., Finkel, R.C., Riebe, C.S., Granger, D.E., Clayton, J.L., King, J.G., Megahan, W.F., 2001. Mountain erosion over 10 yr, 10 k.y., and 10 m.y. time scales. Geology 29, 591–594.

Korup, O., 2003. Landslide induced river disruption—Geomorphic imprints and scaling effects in alpine catchments of South Westland and Fiordland, New Zealand. Unpublished PhD thesis, Victoria University of Wellington.

Korup, O., McSaveney, M.J., Davies, T.R.H., in press. Sediment generation and delivery from large historic landslides in the Southern Alps, New Zealand. Geomorphology.

McKerchar, A.I., Pearson, C.P., 1989. Flood frequency in New Zealand. Publication Hydrology of the Centre 20 (Christchurch, 88 pp.).

Miller, D.J., Benda, L.E., 2000. Effects of punctuated sediment supply on valley-floor landforms and sediment transport. Geological Society of America Bulletin 112, 1814–1824.

Nanson, G.C., Knighton, A.D., 1996. Anabranching rivers: their cause, character and classification. Earth Surface Processes and Landforms 21, 217–239.

Nathan, S., 1978. Upper Cenozoic stratigraphy of South Westland, New Zealand. New Zealand Journal of Geology and Geophysics 21, 329–361.

Nicholas, A.P., Murray, T., Ashworth, P.J., Kirkby, M.J., Macklin, M.G., 1995. Sediment slugs: large-scale fluctuations in fluvial sediment transport rates and storage volumes. Progress in Physical Geography 19, 500–519.

Norris, R.J., Cooper, A.F., 2000. Late Quaternary slip rates and slip partitioning on the Alpine Fault, New Zealand. Journal of Structural Geology 23, 507–520.

Ohmori, H., 1992. Dynamics and erosion rate of the river running on a thick deposit supplied by a large landslide. Zeitschrift für Geomorphologie Supplementband NF 36, 129–140.

Paul, S.K., Bartarya, S.K., Rautela, P., Mahajan, A.K., 2000. Catastrophic mass movement of 1998 monsoons at Malpa in Kali Valley, Kumaun Himalaya, India. Geomorphology 35, 169–180.

Ritter, D.F., Kochel, R.G., Miller, J.R., 1999. The disruption of Grassy Creek: implications concerning catastrophic events and thresholds. Geomorphology 29, 323–338.

Sah, M.P., Mazari, R.K., 1998. Anthropogenically accelerated mass movement, Kulu Valley, Himachal Pradesh, India. Geomorphology 26, 123–138.

Schumm, S.A., 1969. River metamorphosis. American Society of Civil Engineers. Journal of Hydraulics Division HY 1, 255–273.

Shroder Jr., J.F., 1998. Slope failure and denudation in the western Himalaya. Geomorphology 26, 81–105.

Simpson, G.D.H., Cooper, A.F., Norris, R.J., 1994. Late Quaternary evolution of the Alpine Fault zone at Paringa, South Westland, New Zealand. New Zealand Journal of Geology and Geophysics 37, 49–58.

Sutherland, D.G., Ball, M.H., Hilton, S.J., Lisle, T.E., 2002. Evolution of a landslide-induced sediment wave in the Navarro River, California. Geological Society of America Bulletin 114, 1036–1048.

Werritty, A., Leys, K.F., 2001. The sensitivity of Scottish rivers and upland valley floors to recent environmental change. Catena 42, 251–273.

Whitehouse, I.E., 1983. Distribution of large rock avalanche deposits in the central Southern Alps, New Zealand. New Zealand Journal of Geology and Geophysics 26, 272–279.

Yetton, M.D., Wells, A., Traylen, N.J., 1998. The probability and consequences of the next Alpine Fault earthquake. EQC Research Project 95/193. Geotech Consulting Christchurch. 161 pp.

Zarn, B., Davies, T.R.H., 1994. The significance of processes on alluvial fans to hazard assessment. Zeitschrift für Geomorphologie 38, 487–500.